ISSN 0023-1584, Kinetics and Catalysis, 2023, Vol. 64, No. 3, pp. 250–259. © Pleiades Publishing, Ltd., 2023.
Russian Text © The Author(s), 2023, published in Kinetika i Kataliz, 2023, Vol. 64, No. 3, pp. 276–286.

Novel Two-Stage Method of Preparing Graphitic Carbon Nitride Doped by Chlorine for Photocatalytic Hydrogen Evolution and Photocurrent Generation

A. V. Zhurenok[a], D. V. Markovskaya[a], *, K. O. Potapenko[a], N. D. Sidorenko[a], S. V. Cherepanova[a], A. A. Saraev[a], E. Y. Gerasimov[a], and E. A. Kozlova[a]

[a] *Federal Research Center Boreskov Institute of Catalysis, Siberian Branch, Russian Academy of Sciences, Novosibirsk, 630090 Russia*

**e-mail: madiva@catalysis.ru*

Received December 14, 2022; revised January 25, 2023; accepted January 26, 2023

Abstract—In this work, graphitic carbon nitride doped by chlorine was prepared by a two-stage procedure for the first time. At the first stage, melamine was hydrothermally treated with glucose; at the second stage, the resulting precursor was calcined in a mixture with ammonium chloride. The obtained samples were studied using a set of physicochemical methods, such as X-ray diffraction (XRD) analysis, transmission electron microscopy (TEM), scanning electron microscopy (SEM), X-ray photoelectron spectroscopy (XPS), diffuse reflectance spectroscopy, and photoelectrochemical methods. All of the synthesized photocatalysts were tested in the reaction of photocatalytic hydrogen production from basic solutions of triethanolamine. The highest rates of hydrogen evolution and short-circuit current densities were obtained with a photocatalyst prepared by the calcination of a mixture consisting of 30% ammonium chloride and 70% melamine. The catalytic activity of this sample was 1332 μmol h^{-1} g^{-1}, and it was higher than the catalytic activity of carbon nitride prepared by the calcination of melamine without pretreatment by a factor of 22.

Keywords: carbon nitride, chlorine doping, hydrogen production, photocatalysis, photocurrent, visible light

DOI: 10.1134/S0023158423030114

Abstract—In this study, a cocatalyst is supported on the surface of carbon nitride by the following three different methods: thermal phosphorylation, a hydrothermal method, and photochemical reduction. In the first case, the cocatalyst is a cobalt phosphide–cobalt orthophosphate mixture; the use of the hydrothermal and photochemical synthesis methods provides the formation of cobalt orthophosphate. In addition, a sample is synthesized by a hydrothermal treatment of presynthesized carbon nitride and cobalt phosphide. The synthesized samples are studied using the following set of physicochemical methods: X-ray diffraction (XRD) analysis, transmission electron microscopy (TEM), X-ray photoelectron spectroscopy (XPS), and diffuse reflectance spectroscopy. All the synthesized photocatalysts are tested in photocatalytic hydrogen evolution from an aqueous alkaline solution of triethanolamine and in a photoelectrochemical cell containing a sodium polysulfide solution. It is shown that, in the case of using a cobalt phosphide–cobalt orthophosphate mixture, the target characteristics are higher than those in the case of cobalt orthophosphate and carbon nitride. The highest catalytic activity is 156 mol h^{-1} g^{-1}; it is comparable to the activity of platinized carbon nitride. The highest short-circuit current density obtained in the case of using a photoelectrode containing cobalt phosphide and cobalt phosphate is 2.4 mA/cm^2.

Abbreviations and notation: XRD, X-ray diffraction; TEM, transmission electron microscopy; SEM, scanning electron microscopy; XPS, X-ray photoelectron spectroscopy; CSR, coherent scattering region; BET, Brunauer–Emmett–Teller method.

INTRODUCTION

The widespread development of alternative energy and energy generation processes using the most environmentally friendly methods is of considerable current importance for modern society [1]. From this point of view, it is reasonable to consider hydrogen as a fuel. Hydrogen has the highest specific heat of combustion; in this case, water is released, and it does not have a harmful effect on the environment. In addition, hydrogen is one of the most common elements on the Earth; because of this, various compounds, ranging from the simplest hydrocarbons and water to complex mixtures like biomass, can be used to obtain hydrogen [2]. It should be noted that the infrastructure for transporting hydrogen to the place of consumption is simi-

lar to the infrastructure used for gas transportation [1]. Thus, researchers are facing problems of the synthesis and storage of hydrogen. Particular attention should be paid to methods that make it possible to obtain hydrogen not only on an industrial scale but also on a smaller scale for local consumption or in remote places.

From this point of view, the photocatalytic decomposition of water and aqueous solutions of organic and inorganic substances is a promising method. The mechanisms of photocatalysis make it possible to combine the synthesis of hydrogen and the decomposition of impurities, which contributes to additional purification of water [1, 3, 4]. The most common photocatalysts are semiconductor materials that are active to the action of visible light, which is the major portion of the solar spectrum [5–10]. Currently, researchers are actively studying carbon-containing materials, such as graphitic carbon nitride [11, 12]. Carbon nitride has a high electronic conductivity; it is resistant to acids and alkalis and is stable over a wide temperature range [11, 12]. However, this photocatalyst has two fundamental drawbacks, which seriously limit its practical application: a low specific surface area and a high rate of recombination of electron–hole pairs [13–21]. The specific surface area can be increased by synthesizing in the presence of templates [13, 14]. The combustion of these compounds results in the formation of an ordered and developed catalyst texture, which is reflected in larger surface areas and pore volumes of the materials. The rate of recombination of electron–hole pairs can be decreased by changing the electronic structure of the semiconductor. For this purpose, methods that have previously proven their effectiveness with respect to other semiconductor catalysts are used, the simplest of which is the doping of carbon nitride with foreign metal and nonmetal ions [15, 16]. A significant disadvantage of the use of metals is the low stability of the resulting photocatalysts and the possibility of changing the degree of oxidation of metals under the influence of temperature in the course of the preparation and operation of photocatalysts [17]. For this reason, doping with nonmetals is used more widely. The greatest number of publications was devoted to the incorporation of boron, phosphorus, and fluorine into the structure of carbon nitride [18–21]. Doping with other halogens, such as chlorine, has been studied to a much lesser extent. However, chlorine is characterized by high electronegativity, which leads to the strongest changes in the electronic structure of semiconductors upon doping. Therefore, photocatalysts based on carbon nitride doped with chlorine atoms are interesting test materials. Note that, at present, researchers rarely combine both approaches in a synthesis to improve the characteristics of carbon nitride [22]. In this regard, the aim of this work was to study photocatalysts based on chlorine-doped carbon nitride obtained by a two-stage synthesis procedure, which makes it possible to simultaneously improve the texture and electronic properties of the catalyst.

EXPERIMENTAL

Preparation of Photocatalysts

Photocatalysts were synthesized by the thermal polymerization of melamine, which was subjected to hydrothermal pretreatment. At the first stage, a mixture consisting of 15 g of melamine, 104 mg of D-glucose, and water was treated in an ultrasonic bath; thereafter, it was placed in an autoclave at a temperature of 180°C for 12 h (the autoclave filling factor was 60%) [23]. The precipitate formed was washed several times with water and ethanol and dried in a flow of air at 60°C for 4 h. At the second stage, a mixture of melamine and ammonium chloride with a total weight of 2 g was calcined at 550°C for 2 h [24]. The resulting samples were washed and dried similarly to those prepared at the first stage of the synthesis. The photocatalysts prepared by this procedure are denoted in the text as *y*% NH_4Cl, where *y* is the weight concentration of ammonium chloride in the mixture before calcination.

To carry out photocatalytic tests, 1 wt % platinum was supported onto the surface of samples by the chemical reduction of chloroplatinic acid with sodium borohydride [24].

Study of the Physicochemical Properties of Samples

The X-ray diffraction patterns were measured on a Bruker D8 X-ray diffractometer (Bruker, Germany) with CuK_α radiation (the wavelength $\lambda = 1.5418$ Å). The spectra were recorded in the angle range $2\theta = 15°–65°$ by point-by-point scanning with a scanning step of 0.05°; the accumulation time per point was 10 s. The diffuse reflectance spectra were recorded on a UV-250 spectrophotometer (Shimadzu, Japan) equipped with an ISR-240A diffuse reflectance attachment. The measurements were carried out in a wavelength range from 250 to 800 nm; barium sulfate was used as a reference sample. The textural characteristics of the photocatalysts were determined by low-temperature nitrogen adsorption on an Autosorb-6B instrument (Quantachrome, the United States). The chemical composition of the samples was studied using X-ray photoelectron spectroscopy (XPS) on a SPECS electron spectrometer from Surface Nano Analysis GmbH (Germany). The spectrometer was equipped with a PHOIBOS-150-MCD-9 hemispherical analyzer and an XR-50 source of characteristic X-ray radiation with a double Al/Mg anode. The spectra were recorded using nonmonochromatic AlK_α radiation ($h\upsilon = 1486.61$ eV). Data processing was performed using the CasaXPS software package. The shape of peaks was approximated by a symmetric function obtained by summing the Gaussian and Lorentzian functions. The microstructure of the pho-

Table 1. Main physicochemical properties of the prepared photocatalysts

$w(NH_4Cl)$, %	L_a, nm	L_c, nm	E_g, eV	λ, nm	S_{BET}, m^2/g	V_{pore}, cm^3/g
0	5.9	5.3	2.7 ± 0.1	457 ± 20	11.2	0.05
5	5.9	5.3	2.75 ± 0.07	451 ± 11	21.9	0.09
10	4.4	4.7	2.8 ± 0.2	451 ± 24	20.1	0.10
20	4.2	4.8	2.8 ± 0.1	448 ± 16	20.7	0.14
30	4.4	4.9	2.77 ± 0.08	448 ± 13	25.7	0.16
40	4.6	4.5	2.78 ± 0.09	446 ± 15	30.2	0.19
50	4.2	3.6	2.8 ± 0.1	446 ± 18	32.3	0.22

$w(NH_4Cl)$ is the percentage of ammonium chloride in the calcinations mixture; L_a is the CSR in the plane of the layer; L_c is the CSR in the plane perpendicular to the plane of the layer; E_g is the band gap; λ is the absorption edge; S_{BET} is the surface area; and V_{pore} is the pore volume.

tocatalysts was studied by scanning electron microscopy using a ThemisZ microscope (Thermo Fisher Scientific, the United States) with an accelerating voltage of 200 kV. The micrographs were taken with a Ceta 16 CCD sensor (Thermo Fisher Scientific, the United States).

The photoelectrochemical properties of the samples were studied in a two-electrode cell. An FTO conductive glass, onto the surface of which 30 mg of a photocatalyst was supported by droplet deposition, was used as a working electrode. The counter electrode was brass coated with copper(I) sulfide. The measurements were carried out on a P-45Kh potentiostat–galvanostat (Russia) with an FRA-24M electrochemical impedance measurement module in an electrolyte solution prepared by adding an equimolar amount of sulfur and sodium chloride (0.1 M) to 1 M solution of sodium sulfide. To improve contacts, the electrodes were compressed. The photoelectrochemical cell was illuminated with a 425 LED (radiation power, 20 mW/cm^2). All samples were studied by cyclic voltammetry (potential sweep rate, 0.02 V/s; potential range, from –0.8 to 0.8 V), impedance spectroscopy (frequencies, 0.8–10^5 Hz; amplitude, 10 mV; potential, 200 mV), and the Mott–Schottky method (potential range, from –0.6 to 0.6 V; amplitude, 10 mV; frequency, 1000 Hz).

Measurement of Catalytic Activity

The photocatalytic properties of the synthesized samples were studied in the reaction of hydrogen evolution from aqueous alkaline solutions of triethanolamine. The reaction mixture of 10 vol % triethanolamine, 0.1 M sodium hydroxide, and 50 mg of a photo catalyst was purged with argon until oxygen was completely removed and then illuminated for 2 h using a LED with a wavelength of 425 nm and a radiation power of 20 mW/cm^2. The amount of produced hydrogen was determined by gas chromatography (Khromos, Russia); samples were taken at regular intervals of 15 min. The catalytic activity was calculated from the slope of the linear part of a kinetic curve.

RESULTS AND DISCUSSION

Physicochemical Properties of the Prepared Catalysts

The prepared photocatalysts were studied using a set of physicochemical methods; Table 1 summarizes the main characteristics of the samples. The phase composition of the photocatalysts was studied by XRD analysis. Figure 1 shows the experimental XRD patterns. The XRD patterns of the samples exhibited two peaks at 13° (the (100) plane) and 27° (the (002) plane), which are characteristic of a graphitic carbon nitride phase. The position of the peak at 27° (the crystallographic plane (002), Table 1) shifted depending on the concentration of ammonium chloride added at the stage of reaction mixture preparation, and this shift can indicate the incorporation of chlorine atoms into the structure of carbon nitride. Additionally, the characteristic dimensions of the layered material in two directions were calculated: L_a is the distance between the tri-*s*-triazine units of the polymer, and L_c is the distance between the polymer layers in the plane perpendicular to the layer in which the tri-*s*-triazine units are located [24]. Table 1 summarizes the results. In general, there were tendencies toward a decrease in the characteristic distances L_a and L_c with the amount of ammonium chloride introduced into the structure. This was especially pronounced in the samples containing to 20% ammonium chloride in a mixture for calcinations. The parameter L_a took an approximately constant value of 4.2–4.6 nm for the samples in which the ammonium chloride concentration varied from 30 to 50%. This may be related to either the amount of chlorine introduced into the structure or the formation of a porous structure upon the burning out of ammonium chloride as a template.

The optical properties of the photocatalysts were studied by diffuse reflectance spectroscopy. Figure 2 shows the corresponding spectra. All samples absorbed light in the visible region, and they were

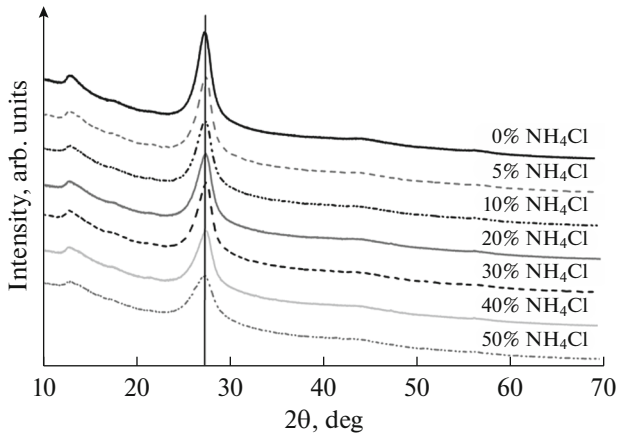

Fig. 1. X-ray diffraction patterns of photocatalysts obtained by the calcination of mixtures with different weight concentrations of ammonium chloride *y*% NH_4Cl.

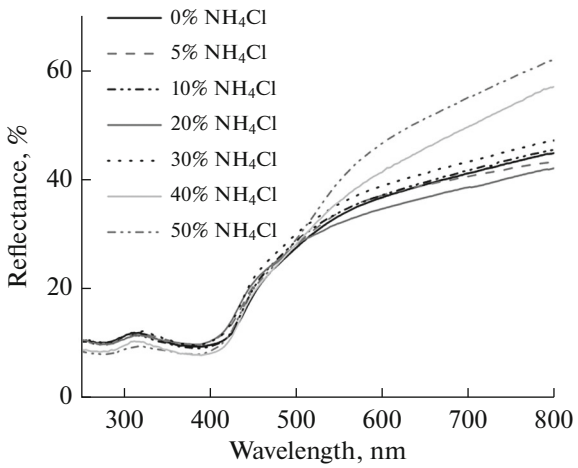

Fig. 2. Diffuse reflectance spectra of photocatalysts *y*% NH_4Cl.

potentially active photocatalysts and electrodes. The absorption edge and band gap of photocatalysts were calculated from diffuse reflectance spectroscopy data (Table 1). It should be noted that the band gap for the entire series of samples was in a range of 2.7–2.8 eV. The absorption edge of carbon nitride was 457 nm, and this value is consistent with published data [25–28]. The addition of ammonium chloride to melamine at the stage of catalyst preparation did not change the absorption edge or band gap of the photocatalysts. This was, probably, due to a low chlorine weight content of the samples, which did not affect their optical properties.

The textural properties of the samples were studied by the low-temperature adsorption of nitrogen. The specific surface area of carbon nitride obtained by annealing melamine after hydrothermal treatment was low and amounted to 11.2 m^2/g (Table 1). The addition of 5 wt % ammonium chloride to melamine made it possible to increase this value by a factor of 2. In the case of samples prepared by the calcination of a mixture containing to 20% ammonium chloride, the surface area of the material remained constant. However, a further increase in the amount of this additive led to a linear increase in the surface area of carbon nitride. Such an effect of ammonium chloride on the surface area was due to the fact that the ammonium salt acted as a template under these conditions. Thermal decomposition of NH_4Cl proceeds at lower temperatures than that of melamine; because of this, material with an ordered texture and higher target characteristics can be obtained. Indirectly, this is evidenced by the data given in Table 1 on changes in the pore volume of carbon nitride: the pore volume of carbon nitride increased with the amount of ammonium chloride added to melamine. Note that higher surface areas and pore volumes are favorable for the occurrence of photocatalytic reactions.

The photocatalysts prepared from mixtures containing 0–50% ammonium chloride were additionally studied by XPS. Figures 3a–3c show the experimental spectra. The C 1*s* spectrum (Fig. 3a) is adequately described by two peaks: the first one with a binding energy (E_b) of 284.8–285.2 eV corresponds to an sp^2-hybridized carbon atom and indicates the presence of a C=C double bond [29–32], and the second peak with E_b = 288.1 eV indicates the presence of N–C=N bonds with nitrogen atoms [29–32]. Figure 3b shows that the N 1*s* spectrum exhibited four peaks with binding energies at 398.6, 400.0, 401.0, and 404.4 eV. According to published data, the first peak was due to the nitrogen atoms that form the C–N=C bond in a tri-*s*-triazine ring [29–32], the second was due to the N atom bonded to three $N-(C)_3$ carbon atoms [29, 30, 32], and the third was due to terminal N–H groups [29–32]. The fourth peak corresponded to an excited π bond [33]. From the results of quantitative analysis (Table 2), it follows that the concentration ratio between nitrogen and carbon atoms on the surface was nearly stoichiometric. Figure 3c shows the spectra of platinum for the tested photocatalysts. All of them were a superposition of two peaks: platinum in a metallic state with a binding energy of 70.7–71.0 eV [34, 35] and platinum in the oxidized state Pt^{2+} (E_b = 72.9 eV) [36–39]. As shown in Table 2, the fraction of metallic platinum in the tested catalysts was at least 82%. Previously, it was found that platinum in a metallic form increased the rate of photocatalytic hydrogen evolution [40].

It should be noted that no peaks corresponding to chlorine atoms were found in the spectra of all samples. This can be related to its concentration on the surface lower than the limit of detection because of the incorporation of chlorine into the bulk structure of the semiconductor. This fact indirectly indicates that ammonium chloride acted as a template in this syn-

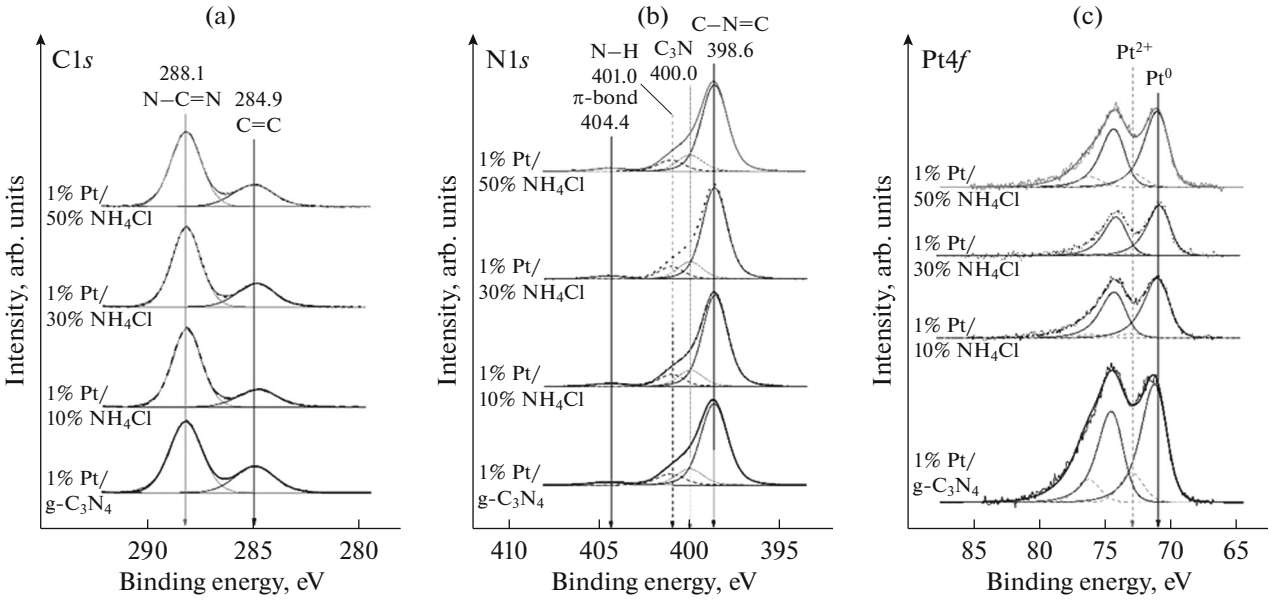

Fig. 3. XPS spectra of 1% Pt/g-C_3N_4, 1% Pt/10% NH_4Cl, 1% Pt/30% NH_4Cl, and 1% Pt/50% NH_4Cl photocatalysts: (a) C 1*s*, (b) N 1*s*, and (c) Pt 4*f* lines.

thesis method, and it did not affect the chemical nature of the samples.

To confirm the qualitative composition of the prepared photocatalysts, the samples of 1% Pt/g-C_3N_4 and 1% Pt/30% NH_4Cl were studied by transmission microscopy. As can be seen in Figs. 4a and 4b, the tested samples were flattened cylindrical tubes 10–30 nm thick, on the surface of which spherical particles less than 10 nm in diameter with interplanar spacings of 0.23 and 0.20 nm, corresponding to the reflections (111) and (200) of metallic platinum, were deposited (PDF #000-04-082). For clarity, the platinum particles in Figs. 4a–4c are circled in white. Figure 4c shows a fragment of a cylindrical tube of the 1% Pt/30% NH_4Cl sample with interplanar spacings of 0.33 and 0.52 nm corresponding to the (110) and (100) reflections of graphitic carbon nitride (PDF #000-50-1512). The interplanar spacings differed from the tabulated values within the experimental error, and there was also no increase in the characteristic distance, which could be expected in the case of the introduction of chlorine atoms into the carbon nitride structure.

The 1% Pt/30% NH_4Cl photocatalyst was additionally studied by scanning electron microscopy (SEM). It can be seen in Fig. 5a that the sample consisted of cylindrical agglomerates and plates. Elemental mapping was used to identify the qualitative composition of the analyzed area. Figure 5b shows a distribution map of the main identified elements: carbon, nitrogen, chlorine, and platinum. As follows from Figs. 5c and 5d, carbon and nitrogen were localized in the sample in the same places; this is true for agglomerates of both forms. Thus, the data obtained by TEM and SEM are consistent with each other. Figure 5d shows a distribution map of chlorine. It can be seen that chlorine was uniformly distributed over the surface; a similar conclusion is also valid for platinum deposited on carbon nitride particles. The area marked in Fig. 5a was additionally studied by energy-dispersive spectroscopy, and Table 3 summarizes the quantitative data. As follows from Table 3, the analyzed area of the photo catalyst was formed mainly by carbon and nitrogen atoms. Oxygen, chlorine, and platinum were also present on the surface. Oxygen can occur in the form of carbon dioxide adsorbed on the surface of the photo catalyst, or it can acidify a part of the surface during calcinations, which was carried out in an air flow. Chlorine and platinum were contained in the sample in small amounts of 0.1 and 0.3%, respectively. Thus, scanning electron microscopy and energy-dispersive spectroscopy confirmed the presence of chlorine in the photocatalyst.

Table 2. Quantitative ratios between elements in the photocatalysts measured by XPS

$w(NH_4Cl)$, %	[N]/[C]	[Pt]/[C]	Pt^0, %	Pt^{2+}, %
0	1.40	0.016	82	18
10	1.43	0.007	94	6
30	1.42	0.005	96	4
50	1.41	0.009	86	14

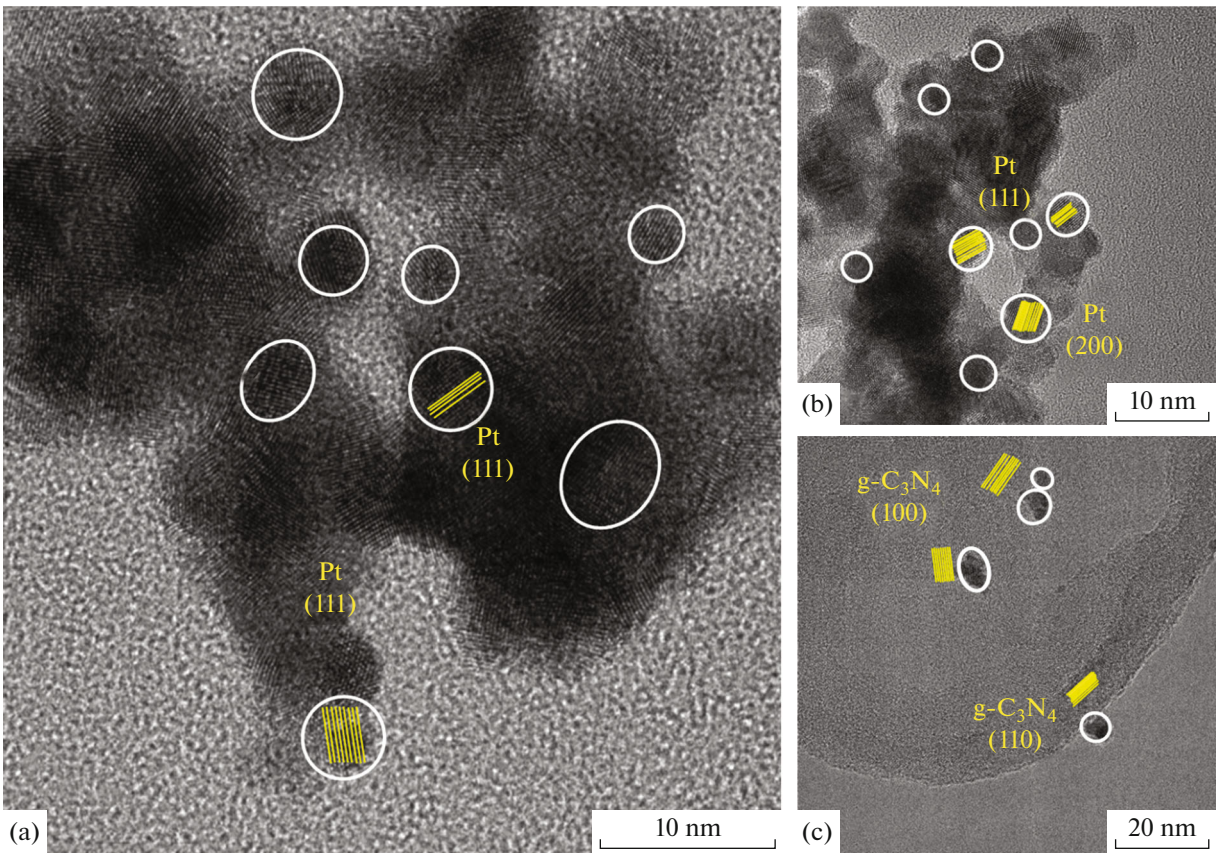

Fig. 4. High-resolution TEM images of (a) 1% Pt/g-C_3N_4 and (b, c) 1% Pt/30% NH_4Cl photocatalysts.

Photocatalytic Properties of the Synthesized Samples

The photocatalytic activity of all prepared samples was studied in the reaction of hydrogen evolution from aqueous alkaline solutions of triethanolamine under visible radiation; Fig. 6a illustrates the experimental data. In the absence of ammonium chloride, the rate of hydrogen evolution W was 276 μmol h^{-1} g^{-1}. The addition of 5 wt % ammonium chloride led to an increase in the rate of reaction by a factor of almost 2. The subsequent increase in the concentration of ammonium chloride in the mixture for calcination to 30% was accompanied by an increase in the catalytic activity to 1332 mol h^{-1} g^{-1}. Most likely, this behavior of the catalyst was related to an increase in the surface area with the ammonium chloride concentration, which made it possible to increase the adsorption of reagents and, hence, the rate of the heterogeneous catalytic reaction. However, a further increase in the weight fraction of ammonium chloride in the mixture for preparing catalysts from 30 to 50% led to a decrease in the rate of photocatalytic hydrogen evolution despite an increase in the catalyst surface area. It is reasonable to assume that these changes in the catalytic activity were associated with the influence of the chemical nature of the resulting photocatalysts. For a detailed consideration of the effect of this factor, we plotted the dependence of the catalytic activity normalized to the catalyst surface area (Fig. 6b) on the weight fraction of NH_4Cl in the reaction mixture at the stage of heat treatment of the photocatalyst. Figure 6b shows that the dependence had a dome-like shape typical of samples doped with various ions, for example, chlorine, the presence of which in the catalysts was confirmed by elemental mapping. The doping of carbon nitride with chloride ions was accompanied by a change in the energy structure of the semiconductor: in this case, the 3*p* orbitals of the halogen formed an impurity energy level in the band gap of

Table 3. Relative weight fractions of elements in the 1% Pt/30% NH_4Cl photocatalyst determined by energy-dispersive spectroscopy

Element	Weight fraction, %
Carbon	50.3
Nitrogen	37.6
Oxygen	11.7
Chlorine	0.1
Platinum	0.3

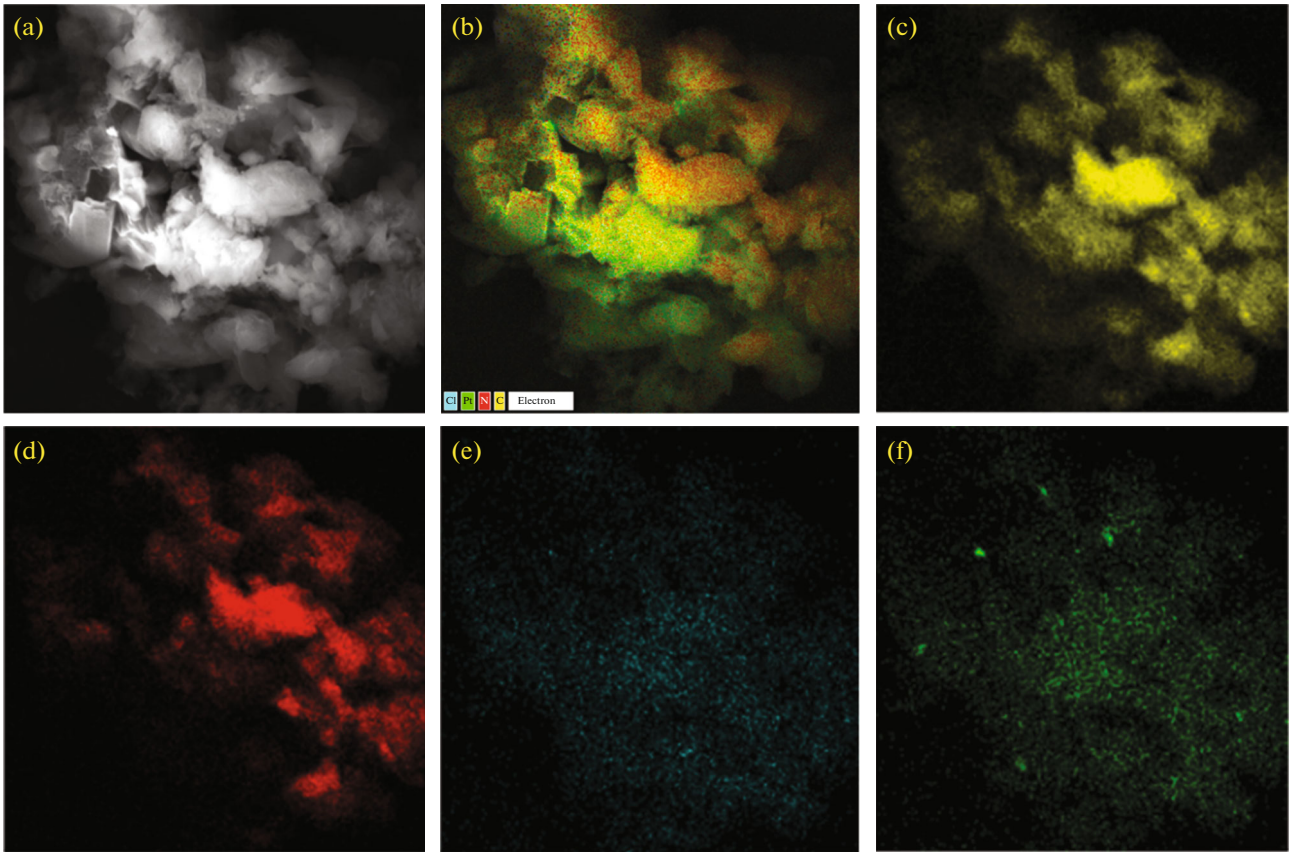

Fig. 5. (a) Scanning electron microscopy image of a 1% Pt/30% NH_4Cl sample and (b–f) the elemental mapping of the SEM image: distribution maps of (b) carbon, nitrogen, chlorine, and platinum; (c) carbon; (d) nitrogen; (e) chlorine; and (f) platinum.

C_3N_4, similarly to that upon the doping of sulfide photocatalysts with transition metal cations [41]. The appearance of such a level promoted the capture of photogenerated charges and an increase in the degree of spatial separation of electron–hole pairs, which led to an increase in catalytic activity [41]. However, an increase in the amount of the introduced ions contributed to the appearance of defects in the carbon nitride structure, which can act as recombination sites at high concentrations to decrease the rate of hydrogen evolution [41]. The maximum catalytic activity was recorded in the testing of a sample for the synthesis of which a mixture of 70% melamine and 30% ammonium chloride was calcined. The value obtained was higher by a factor of 22 than the activity of platinized carbon nitride prepared by calcining melamine without additional processing. Thus, the combination of simultaneous hydrothermal pretreatment with glucose and calcination of melamine with a template capable of incorporating small halogen amounts into the structure is a successful method for increasing the catalytic activity of graphitic carbon nitride by structuring the texture of the photo catalyst and changing its electronic structure.

Photoelectrochemical Properties of the Prepared Photocatalysts

All of the synthesized photocatalysts were deposited onto the conductive glass, and the photovoltaic properties of the resulting electrodes were studied by voltammetry in a two-electrode cell. The short-circuit current density (current density at zero voltage) was chosen to compare the photovoltaic properties of different samples; Table 4 summarizes these values. It can be seen that an increase in the amount of ammonium chloride in the reaction mixture at the stage of catalyst preparation led to an increase in the short-circuit current density, and a maximum value was observed at a 30% concentration of ammonium chloride in the reaction mixture. The subsequent increase in the weight fraction of ammonium chloride was accompanied by a sharp drop in the short-circuit current density. Similar changes in the target properties of photocatalysts depending on the amount of ammonium chloride were observed previously for catalytic activity normalized per unit area.

To test the proposed hypothesis, we studied the photoelectrodes by impedance spectroscopy. Figure 7 shows the obtained data in the Nyquist coordinates. It can be seen that the radii of corresponding hodo-

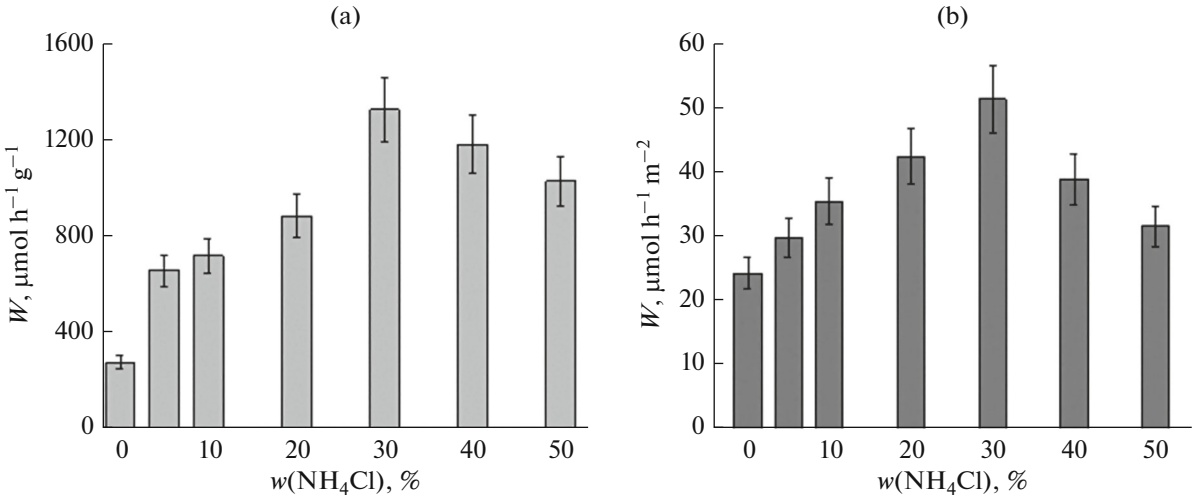

Fig. 6. Dependences of the catalytic activity normalized to (a) the weight of the catalyst and (b) the surface area of the catalyst on the weight fraction of ammonium chloride added in the preparation of the catalysts.

graphs decreased in the same order in which the values of the short-circuit current increased. Thus, the results of voltammetry and impedance spectroscopy are consistent with each other. Additionally, the lifetimes of photogenerated electrons were calculated from the impedance data (Table 4). The dependence of the lifetime of photogenerated electrons, as well as the short-circuit current density and the rate of hydrogen evolution, on the ammonium chloride content of the reaction mixture had a domed shape. The reasons for this behavior of the system will be discussed below.

Additionally, the products of the number of photogenerated electrons in the system and the dielectric constant of the catalyst were estimated from the data obtained by the Mott–Schottky method (Table 4). The dielectric constant was the same for all photocatalysts because all of the catalysts had the same chemical nature. Accordingly, changes in the number of photogenerated electrons in the system can be reliably judged by changes in the product $N \times \varepsilon$, where N is the concentration of electrons moving between electrodes in the photoelectrochemical cell, and ε is the permittivity of the photocatalyst. The data in Table 4 show that the addition of a small amount of ammonium chloride to melamine led to an increase in the electron concentration by a factor of 12. The subsequent increase in the ammonium chloride content of the reaction mixture to 30 wt % had almost no effect on the number of photogenerated electrons: the difference between the parameters $N \times \varepsilon$ for photocatalysts obtained by the calcination of mixtures containing 10 and 30% NH_4Cl did not exceed the experimental error. However, a further increase in the fraction of ammonium chloride from 30 to 50 wt % was accompanied by a sharp drop in the value of this parameter (by almost three orders of magnitude).

It should be taken into account that the introduction of a small amount of chlorine (according to the

Table 4. Photovoltaic properties of prepared samples and the results of measurements by impedance spectroscopy

$w(NH_4Cl)$, %	Short-circuit current density, mA/cm^2	Electron lifetime, ms	$N \times \varepsilon$, m^{-3}
0	0.395	0.79	7.9×10^{18}
5	0.461	1.04	9.5×10^{19}
10	0.677	1.19	1.0×10^{20}
20	0.777	1.21	1.1×10^{20}
30	3.332	2.10	1.3×10^{20}
40	2.398	1.24	2.1×10^{19}
50	1.173	0.98	4.7×10^{17}

N is the concentration of electrons moving between the electrodes of the photoelectrochemical cell; ε is the permittivity of the photo catalyst.

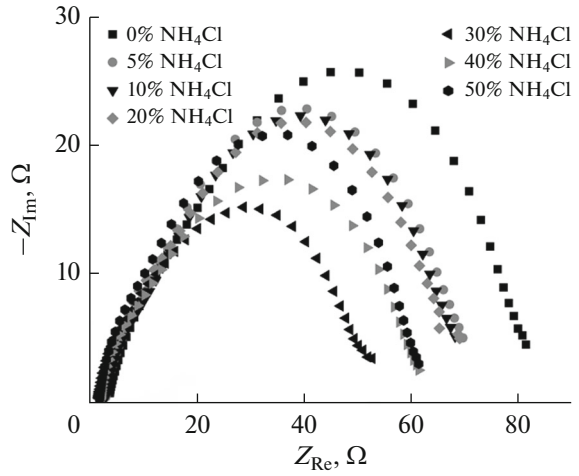

Fig. 7. Impedance hodographs in the Nyquist coordinates obtained for the tested photoelectrodes. Experimental conditions: potential, 0.2 V; potential amplitude, 10 mV; and frequency range, from 0.8 to 10^5 Hz.

energy-dispersive spectroscopy data, it was 0.1% for the most active 30% NH_4Cl photo catalyst) was accompanied by the formation of a new energy level in the semiconductor structure. Summing up the data obtained by the impedance method, we can draw the following conclusions: chlorine doping of carbon nitride with the addition of 5% ammonium chloride led to the formation of a new energy level, and the lifetime of charge carriers can increase due to their movement to this level. For the same reason, their concentration increased. The subsequent increase in the ammonium chloride content of the mixture led to a slight change in the position of this energy level in accordance with the Nernst equation; the number of electrons and the rate of growth of their lifetime were small. The achievement of the optimal position of the energy level and the concentration of defects, which inevitably arise in the semiconductor upon doping, is accompanied by the longest lifetimes and the largest numbers of electrons. In the curves of changes in the target characteristics (the rate of hydrogen evolution and short-circuit current density) as functions of the added amount of ammonium chloride, this moment manifested itself as maximum values of the measured characteristics. A further increase in the ammonium chloride content of the mixture for calcination led to an increase in the amounts of introduced chlorine and defects accompanying this transformation. However, in this case, the defects became recombination sites: both the lifetime and the concentration of electrons decreased. At the same time, the reaction rate and short-circuit current density decreased. Nevertheless, the proposed synthesis procedure makes it possible to achieve good results in improving the target characteristics of carbon nitride: for example, the reference sample obtained by melamine calcination without additional treatments showed a catalytic activity of 60 μmol h^{-1} g^{-1}, and the short-circuit current density was 0.082 mA/cm^2, whereas the target characteristics of the most active photocatalyst were 1332 μmol h^{-1} g^{-1} and 3.332 mA/cm^2, respectively. Thus, the pretreatment of melamine with glucose and its calcination in the presence of ammonium chloride made it possible to improve the catalytic activity and the short-circuit current density by factors of 22 and 41, respectively.

CONCLUSIONS

In this work, we synthesized chlorine-doped carbon nitride by a two-stage procedure, which consisted in the calcination of a mixture of ammonium chloride and melamine previously subjected to hydrothermal treatment in the presence of glucose. The analysis performed using a set of physicochemical methods showed that the procedure proposed makes it possible to obtain chlorine-doped carbon nitride samples with a surface area of 30 m^2/g. The dependences of the rate of photocatalytic hydrogen evolution and the short-circuit current density on the percentage of ammonium chloride in the calcinations mixture were dome-shaped. A sample prepared by the calcinations of a mixture of 70% melamine and 30% ammonium chloride exhibited the highest values of catalytic activity and short-circuit current density (1332 μmol h^{-1} g^{-1} and 3.332 mA/cm^2, respectively). The preliminary treatment of melamine with glucose and its calcination in the presence of ammonium chloride made it possible to improve the catalytic activity and short-circuit current density by factors of 22 and 41, respectively. Thus, the synthesis method proposed is a successful example of improving the target characteristics of graphitic carbon nitride.

ACKNOWLEDGMENTS

We are grateful to PhD E.A. Mel'gunova for the analysis of samples by low-temperature nitrogen adsorption.

FUNDING

This study was supported by the Council for Grants of the President of the Russian Federation for Support of Young Russian Scientists (agreement no. 075-15-2022-435 (MK-2133.2022.1.3)).

CONFLICT OF INTEREST

The authors declare that they have no conflicts of interest.

REFERENCES

1. Hosseini, S.E., Wahid, M.A., Jamil, M.M., Azli, A.A., and Misbah, M.F., *Int. J. Energy Res.,* 2015, vol. 39, p. 1597.

2. Abuadala, A. and Dincer, I., *Int. J. Energy Res.,* 2012, vol. 36, p. 415.
3. Arachchige, S.M. and Brewer, K.J., *Encyclopedia of Inorganic and Bioinorganic Chemistry,* Hoboken, NJ: Wiley, 2011. https://doi.org/10.1002/9781119951438.eibc0458
4. *Heterogeneous Catalysis at Nanoscale for Energy Applications,* Tao, F., Schneider, W.F., and Kamat, P.V., Eds., Hoboken, NJ: Wiley, 2014, p. 326.
5. Acar, C., Dincer, I., and Zamfirescu, C., *Int. J. Energy Res.,* 2014, vol. 38, p. 1903.
6. Zhurenok, A.V., Markovskaya, D.V., Potapenko, K.O., Cherepanova, S.V., Saraev, A.A., Gerasimov, E.Yu., and Kozlova, E.A., *Kinet. Catal.,* 2022, vol. 63, no. 3, p. 248.
7. Markovskaya, D.V., Lyulyukin, M.N., Zhurenok, A.V., and Kozlova, E.A., *Kinet. Catal.,* 2021, vol. 62, no. 4, p. 488.
8. An, C.W., Liu, T., Zhang, D.F., and Yan, J.S., *Kinet. Katal.,* 2020, vol. T. 61, no. 6, p. C. 818.
9. Jain, A. and Ameta, C., *Kinet. Katal.,* 2020, vol. 61, no. 2, p. 246.
10. Krasnyakova, T.V., Yurchilo, S.A., Morenko, V.V., Nosolev, I.K., Glazunova, E.V., Khasbulatov, S.V., Verbenko, I.A., and Mitchenko, S.A., *Kinet. Katal.,* 2020, vol. 61, no. 3, p. 359.
11. Salman, M., Guorui, N., Ayub, Y., Wang, S., Wang, L., Wang, X., Yan, W., Peng, S., and Ramakarishna, S., *Appl. Catal. B: Environ.,* 2019, vol. 257, p. 117855.
12. Koutsouroubi, E.D., Vamvasakis, I., Papadas, I.T., Drivas, C., Choulis, S., Kennou, S., and Armatas, G., *ChemPlusChem,* 2020, vol. 85, p. 1379.
13. Azharal, U., Bashir, M.S., Babar, M., Arif, M., Hassan, A., Riaz, M., Mujahid, R., Sagir, M., Suri, S.U.K., Show, P.L., Chang, J.-S., Khoo, K.S., and Mubashir, M., *Chemosphere,* 2022, p. 134792.
14. Shcherban, N.D., Shvalagin, V.V., Korzhak, G.V., Yaremov, P.S., Skoryk, M.A., Sergiienko, S.A., and Kuchmiy, S.Ya., *J. Mol. Struct.,* 2022, vol. 1250, p. 131741.
15. Patel, S.B., Tripathi, A., and Vyas, A.P., *Environ. Nanotechnol. Monitor. Manage.,* 2021, vol. 16, p. 100589.
16. Lu, S., Shen, L., Li, X., Yu, B., Ding, J., Gao, P., and Zhang, H., *J. Clean. Prod.,* 2022, vol. 378, p. 134589.
17. Zhang, Y., Yuan, J., Ding, Y., Liu, B., Zhao, L., and Zhang, S., *Ceram. Int.,* 2021, vol. 47, p. 31005.
18. Phuc, N.V., An, D.T., Tri, N.N., Tran, H.H., Tran, T.T.H., Nguyen, P.H., and Vien, V.O., *Appl. Mech. Mater.,* 2019, vol. 889, p. 24.
19. Zhou, Y., Zhang, L., Liu, J., Fan, X., Wang, B., Wang, M., Ren, W., Wang, J., Li, M., and Shi, J., *J. Mater. Chem. A,* 2015, vol. 3, p. 3862.
20. Nguyen, M.D., Nguyen, T.B., Thamilselvan, A., Nguyen, T.G., Kuncoro, E.P., and Doong, R.-A., *J. Environ. Chem. Eng.,* 2022, vol. 10, p. 106905.
21. Thorat, N., Yadav, A., Yadav, M., Gupta, S., Varma, R., Pillai, S., Fernandes, R., Patel, M., and Patel, N., *J. Environ. Manage.,* 2019, vol. 247, p. 57.
22. Vasilchenko, D., Zhurenok, A., Saraev, A., Gerasimov, E., Cherepanova, S., Kovtunova, L., Tkachev, S., and Kozlova, E., *Int. J. Hydrogen Energy,* 2022, vol. 47, p. 11326.
23. Sun, S., Li, J., Song, P., Cui, J., Yang, Q., Zheng, X., Yang, Z., and Liang, S., *Appl. Surf. Sci.,* 2020, vol. 500, p. 143985.
24. Zhurenok, A.V., Larina, T.V., Markovskaya, D.V., Cherepanova, S.V., Mel'gunova, E.A., and Kozlova, E.A., *Mendeleev Commun.,* 2021, vol. 31, p. 157.
25. Lu, Y., Wang, W., Cheng, H., Qiu, H., Sun, W., Fang, X., Zhu, J., and Zheng, Y., *Int. J. Hydrogen Energy,* 2022, vol. 47, p. 3733.
26. Skuta, R., Matejka, V., Foniok, K., Smykalova, A., Cvejn, D., Gabor, R., Kormunda, M., Smetana, B., Novak, V., and Praus, P., *Appl. Surf. Sci.,* 2021, vol. 552, p. 149490.
27. Kesavan, G., Vinothkumar, V., Chen, S.-M., and Thangadurai, T.D., *Appl. Surf. Sci.,* 2021, vol. 556, p. 149814.
28. Zhang, Z., Cui, L., Zhang, Y., Klausen, L.H., Chen, M., Sun, D., Xu, S., Kang, S., and Shi, J., *App. Catal. B: Environ.,* 2021, vol. 297, p. 120441.
29. Dong, F., Zhao, Z., Xiong, T., Ni, Z., Zhang, W., Sun, Y., and Ho, W.K., *ACS Appl. Mater. Int.,* 2013, vol. 5, p. 11392.
30. Liu, H., Chen, D., Wang, Z., Jing, H., and Zhang, R., *Appl. Catal. B: Environ.,* 2017, vol. 203, p. 300.
31. Shvalagin, V., Kuchmiy, S., Skoryk, M., Bondarenko, M., and Khyzhun, O., *Mater. Sci. Eng.,* 2021, vol. 271, p. 115304. https://doi.org/10.1016/j.mseb.2021.115304
32. Wang, Z., Wang, Y., Xu, S., Jin, Y., Tang, Z., Xiao, G., and Su, H., *Polym. Degrad. Stabil.,* 2021, vol. 190, p. 109638.
33. Ren, X., Zhang, Y., Yang, L., and Chen, Z., *Inorg. Chem. Commun.,* 2021, vol. 133, p. 108863.
34. Zhurenok, A.V., Markovskaya, D.V., Gerasimov, E.Yu., Cherepanova, S.V., Bukhtiyarov, A.V., and Kozlova, E.A., *RSC Adv.,* 2021, vol. 11, p. 37966.
35. Zhurenok, A.V., Markovskaya, D.V., Gerasimov, E.Yu., Vokhmintsev, A.S., Weinstein, I.A., Prosvirin, I.P., Cherepanova, S.V., Bukhtiyarov, A.V., and Kozlova, E.A., *Catalysts,* 2021, vol. 11, p. 1340.
36. Barr, T.L., *J. Phys. Chem.,* 1978, vol. 82, p. 1801.
37. Bernsmeier, D., Sachse, R., Bernicke, M., Schmack, R., Kettemann, F., Polte, J., and Kraehnert, R., *J. Catal.,* 2019, vol. 369, p. 181.
38. Golabiewska, A., Lisowski, W., Jarek, M., Nowaczyk, G., Zielinska-Jurek, A., and Zaleska, A., *Appl. Surf. Sci.,* 2014, vol. 317, p. 1131.
39. Smirnov, M.Yu., Vovk, E.I., Nartova, A.V., Kalinkin, A.V., and Bukhtiyarov, V.I., *Kinet. Catal.,* 2018, vol. 59, no. 5, p. 653.
40. Kozlova, E.A., Markovskaya, D.V., Cherepanova, S.V., Saraev, A.A., Gerasimov, E.Y., Perevalov, T.V., Kaichev, V.V., and Parmon, V.N., *Int. J. Hydrogen Energy,* 2014, vol. 39, p. 18758.
41. Markovskaya, D.V., Kozlova, E.A., Cherepanova, S.V., Kolinko, P.A., Gerasimov, E.Y., and Parmon, V.N., *ChemPhotoChem,* 2017, vol. 1, p. 575.

Translated by V. Makhlyarchuk